

# Solamargine induces autophagy-mediated apoptosis and enhances bortezomib activity in multiple myeloma

Qiaoyan Han<sup>1,2</sup> | Hua Bai<sup>1</sup> | Yong Xu<sup>1</sup> | Min Zhou<sup>1</sup> | He Zhou<sup>1</sup> |  
Xiaoqing Dong<sup>1</sup>  | Bing Chen<sup>1</sup> 

<sup>1</sup>Department of Hematology, Nanjing Drum Tower Hospital Clinical College of Nanjing University of Chinese Medicine, Nanjing, China

<sup>2</sup>Department of Hematology, Jingjiang People's Hospital, Jingjiang, China

## Correspondence

Xiaoqing Dong and Bing Chen, Department of Hematology, Nanjing Drum Tower Hospital Clinical College of Nanjing University of Chinese Medicine, Nanjing 210008, Jiangsu, China.

Email: [qgswns@126.com](mailto:qgswns@126.com) (X.D.) and [chenbing2004@126.com](mailto:chenbing2004@126.com) (B.C.)

## Funding information

Jiangsu Provincial Medical Innovation Team, Grant/Award Number: CXTDA2017046; Nanjing Medical Science and Technique Development Foundation, Grant/Award Number: YKK20083; National Natural Science Foundation of China, Grant/Award Number: 82000215; Natural Science Foundation of Jiangsu Province, Grant/Award Number: BK20210028

## Abstract

Multiple myeloma (MM) is an incurable plasma cell malignancy with a poor survival rate. Conventional chemotherapeutic agent-induced adverse events, including toxicity, neuropathy or drug resistance, significantly decrease the patients' quality of life and can even lead to interruption of treatment. Therefore, novel therapeutic drugs and strategies are urgently needed to improve MM therapy and patient outcomes. Here, we show that solamargine (SM), a steroidal alkaloid glycoside isolated from a Chinese herb *Solanum nigrum* L., exhibits promising anti-MM activity. In particular, SM suppressed the viability of MM cell lines (ARP-1 and NCI-H929) in a concentration- and time-dependent manner, inducing apoptosis in these cells. RNA-seq analysis showed that treatment with SM led to the upregulation of genes associated with cell death and autophagy in H929 cells. Further, we found that treatment with SM activated autophagy in the MM cells, as incubation with 3-Methyladenine, an inhibitor of autophagy, significantly alleviated SM-triggered apoptosis and inhibition of viability in MM cells. Interestingly, we also observed a synergistic effect between SM and bortezomib (BTZ), a common chemotherapeutic agent for MM, in both MM cells and human bone marrow CD138+ primary myeloma cells. We also confirmed the single-agent efficacy of SM and the synergistic effects between SM and BTZ in an MM xenograft mouse model. Collectively, these findings indicate that SM exerts an anti-MM effect, at least in part, by activating cell autophagy and reveal that SM alone or in combination with BTZ is a potential therapeutic strategy for treating MM.

## KEYWORDS

apoptosis, autophagy, bortezomib, multiple myeloma, solamargine

## 1 | INTRODUCTION

Multiple myeloma (MM) is a haematological malignancy characterised by abnormal proliferation of monoclonal plasma cells in the bone marrow, resulting in excessive secretion of monoclonal immunoglobulin,

**Abbreviations:** 3-MA, 3-methyladenine; ACD, autophagic cell death; BM-MNCs, bone marrow mononuclear cells; BTZ, bortezomib; CCK-8, Cell Counting Kit-8; MM, multiple myeloma; RNA-seq, RNA sequencing; SM, solamargine.

Qiaoyan Han, Hua Bai, and Yong Xu contributed equally to this work.

This is an open access article under the terms of the [Creative Commons Attribution-NonCommercial-NoDerivs](https://creativecommons.org/licenses/by-nc-nd/4.0/) License, which permits use and distribution in any medium, provided the original work is properly cited, the use is non-commercial and no modifications or adaptations are made.

© 2022 The Authors. *Clinical and Experimental Pharmacology and Physiology* published by John Wiley & Sons Australia, Ltd.

leading to organ dysfunction.<sup>1</sup> Over 32,000 patients are newly diagnosed with MM in the United States every year, accounting for about 1% of all cancers and 10% of neoplastic haematologic tumours.<sup>2,3</sup> The survival of these patients has improved dramatically with the development of various novel treatment options, such as immuno-modulatory drugs, proteasome inhibitors, monoclonal antibodies and histone deacetylase inhibitors.<sup>4,5</sup> However, adverse events, including toxicity, neuropathy or relapse are still problems that severely restrict the treatment of MM.<sup>6</sup> Indeed, MM is still considered incurable, and almost 13,000 patients die of this disease each year in the United States.<sup>3</sup> Therefore, there is an urgent demand for new drugs and therapeutic strategies to improve the survival outcomes of MM patients.

Traditional Chinese medicine and its bioactive components play an important role in the treatment of many haematologic tumours. Clinically, homoharringtonine, arsenic trioxide and etoposide have shown potent anti-cancer activity against acute myeloid leukaemia, acute promyelocytic leukaemia and Burkitt Lymphoma.<sup>7-9</sup> For the treatment of MM, some phytochemicals, including agaricus and curcumin, have also been found to exert significant anti-tumour effects by arresting the cell cycle, promoting anti-angiogenesis, or inducing apoptosis.<sup>6</sup> Thus, it is possible that components of natural plants, when extracted, could be used to treat MM and other haematologic

tumours. Solamargine (SM, Figure 1A), a steroidal alkaloid glycoside isolated from the Chinese herb *Solanum nigrum* L., exhibits a promising anti-proliferative activity in various types of cancer cells, including those derived from human gastric cancer, lung cancer and nasopharyngeal carcinoma.<sup>10-12</sup> Nevertheless, the efficacy of SM in the treatment of MM has yet to be evaluated. In addition, while combination chemotherapy with multiple drugs is commonly used in the clinic to improve response rates, prolong response and delay the onset of drug resistance of tumour cells, the efficacy of SM in combination with other anti-MM agents has also not yet been examined.

Among the pathways by which many chemotherapy agents function, autophagy is an evolutionarily conserved intracellular degradation pathway in which protein aggregates and damaged organelles are removed via lysosomal degradation.<sup>13</sup> Autophagy is associated with cell survival/proliferation and is indeed beneficial for tumour maintenance, as it can recycle damaged organelles, overcome nutrient deprivation, relieve metabolic stress, and regulate cellular homeostasis.<sup>14,15</sup> However, excessive autophagy may result in cell death.<sup>16</sup> In MM, autophagy induced by chemotherapeutic drugs can either play a pro-survival and drug-resistant role by relieving cellular stress caused by toxic stimulation, or a subversive role by triggering autophagic cell death (ACD).<sup>17</sup> Thus, regulating autophagy to promote MM cell death

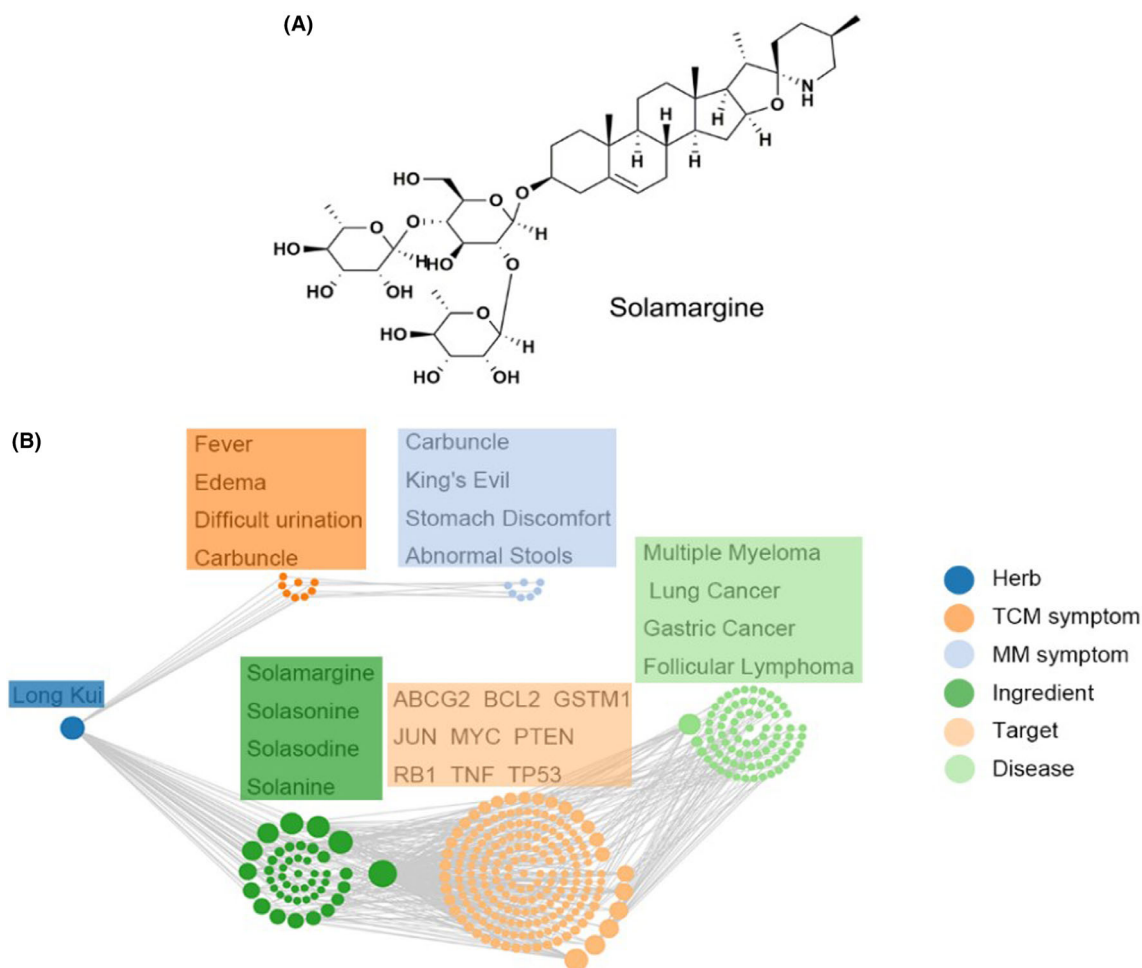


**FIGURE 1** Chemical structure of solamargine (SM) (A) and traditional Chinese medicine symptom-Chinese medicine-target network of SM (B)

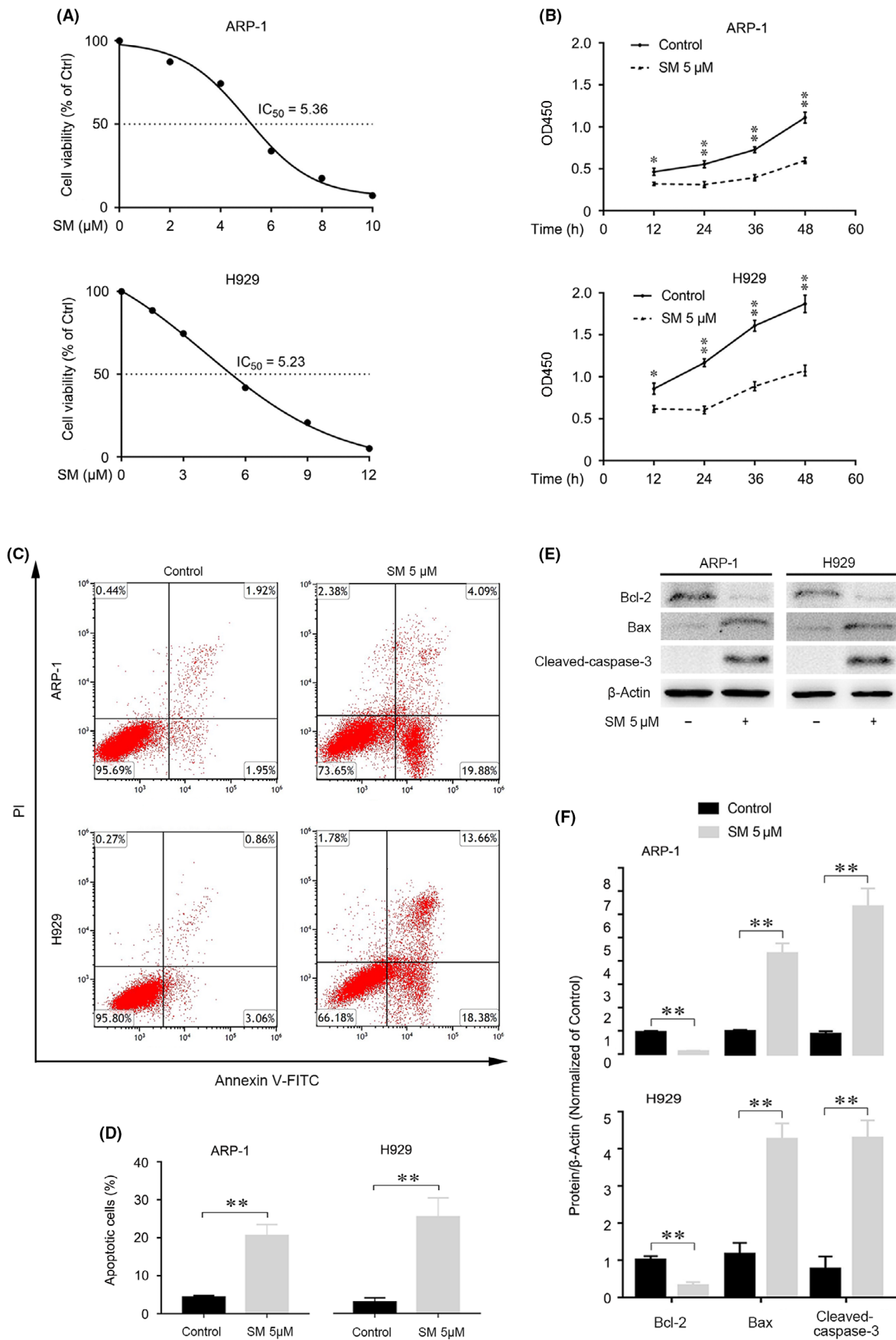


FIGURE 2 Legend on next page.

and increase drug sensitivity may be a novel therapeutic strategy to combat this disease.<sup>18</sup>

In the current study, we investigated the role of SM in the regulation of autophagy in MM cells and the efficacy of this natural agent at suppressing MM *in vitro* and *in vivo*. Furthermore, treatment with SM was combined with bortezomib (BTZ), a chemotherapeutic agent commonly used in the treatment of MM, to investigate this potential clinical application of SM in treating MM. We show for the first time that SM activates autophagy which contributes to apoptosis and suppression of viability in human MM cells (ARP-1 and H929). Moreover, the combination of SM and BTZ exhibits more effective tumour suppression than the treatment of SM or BTZ alone. Our findings thus identify SM, and particularly its combination with BTZ, as potential therapeutic options for the treatment of MM, and provide a theoretical basis for the potential clinical application of SM in MM therapy.

## 2 | RESULTS

### 2.1 | SM suppresses cell viability and induces apoptosis in MM cells

It has been reported that SM suppresses the progression of lung cancer, gastric cancer and nasopharyngeal carcinoma,<sup>10–12</sup> whereas, to our knowledge, the effects of SM on MM has yet to be investigated. We first examined for the potential of SM in treating MM using SymMap, which identifies overlap between known effects of traditional Chinese medicine components and a wide range of diseases.<sup>19</sup> Indeed, this analysis identified some overlap between SM and MM (Figure 1B). Based on this, as well as the known efficacy of SM on other cancers, we investigated the effects of SM on MM cell lines. In particular, we examined the effects of SM at different concentrations on the viability of two MM cell lines, ARP-1 and H929 cells, after incubation for 24 h using the Cell Counting Kit-8 (CCK-8) assay. As shown in Figure 2A, SM inhibited cell viability in a concentration-dependent manner in both ARP-1 and H929 cells, with IC<sub>50</sub> values of 5.36  $\mu$ M and 5.23  $\mu$ M, respectively. Based on this, we examined the effects of SM on these cells at a concentration of 5  $\mu$ M in subsequent experiments. We examined the time-dependent effects of SM on both cells and found a significant decrease in the OD values (at 450 nm) at all time points (Figure 2B). Thus, SM indeed inhibits the viability of MM cells.

To further demonstrate the anti-MM effect of SM, cell apoptosis was measured by flow cytometry, following annexin-V-FITC/PI

staining. As shown in Figure 2C and D, SM treatment for 24 h elicited a significant increase in the relative number of apoptotic ARP-1 and H929 cells. Consistent with this, using Western blotting, we observed robust cleavage of caspase-3, overexpression of Bax and down-regulation of Bcl-2 induced by SM in the cells (Figure 2E and F). These findings clearly demonstrate that SM triggers apoptosis in MM cells.

### 2.2 | SM upregulates genes associated with cell death and autophagy in SM-treated H929 cells

To further characterise the effects of SM on MM cells, we examined the consequences of SM on the global transcriptional programme of H929 cells by performing RNA-seq. After first confirming a high correlation between biological replicates (Figure 3A), we identified 667 differentially expressed genes in cells treated with SM from control cells, including 547 upregulated and 120 downregulated genes (Figure 3B). Gene ontology (GO) analysis identified a wide range of upregulated pathways, including cell death (blue box), consistent with the aforementioned effects of SM on cell viability (Figure 3C). Interestingly, we also found that autophagy-related genes (red box) were dramatically upregulated in H929 cells treated with SM, suggesting that autophagy pathway may be involved in SM-induced suppression of MM.

### 2.3 | SM-induces apoptosis and suppression of viability in MM cells via autophagy

To determine whether indeed treatment with SM triggers autophagy in MM cells, we performed Western blot analysis, examining for the expressions of two autophagy-related proteins LC3-II and Beclin 1. We found that, consistent with the RNA-seq analysis, LC3-II and Beclin 1 were both significantly upregulated by SM in ARP-1 and H929 cells (Figure 4A and B). We then examined the effects of a 2 h pre-treatment with 3-methyladenine (3-MA) (10  $\mu$ M), an inhibitor of autophagy, followed by exposure to SM for 24 h in MM cells. As shown in Figure 4C and D, treatment with 3-MA substantially attenuated the amount of LC3-II, Beclin I, Bax and cleaved-caspase-3 that were enhanced by SM treatment. In contrast, SM-inhibited Bcl-2 was markedly reduced by 3-MA treatment. Furthermore, we found that the negative effects of SM on cell viability were almost completely alleviated by pre-treatment with 3-MA (Figure 4E). These results indicate that inhibition of autophagy by 3-MA rescues MM cells from SM-induced apoptosis and suppression of viability, suggesting that

**FIGURE 2** Solamargine (SM) suppresses cell viability and induces apoptotic death in ARP-1 and H929 cells. ARP-1 and H929 cells were treated with indicated concentrations of SM for 24 h, or treated with 5  $\mu$ M SM for 12–48 h. A and B, Cell viability and the OD values at 450 nm were assessed by CCK-8 assay. The curves of cell viability (A) and the OD<sub>450</sub> values (B) were generated. (C) The percentages of live (the third quadrant), early apoptotic (the fourth quadrant), late apoptotic (the first quadrant) and necrotic cells (the second quadrant) were determined by FACS using annexin-V-FITC/PI staining. The results from a representative experiment are shown. (D) Quantitative analysis of apoptotic cells by FACS assay. (E) Total cell lysates were subjected to Western blotting using indicated antibodies. The blots were probed for  $\beta$ -Actin as a loading control. Similar results were observed in three independent experiments. (F) The blots for Bcl-2, Bax and cleaved-caspase-3 were semi-quantified. All quantified data were expressed as mean  $\pm$  SD (n = 3–5, \*p < 0.05, \*\*p < 0.01)

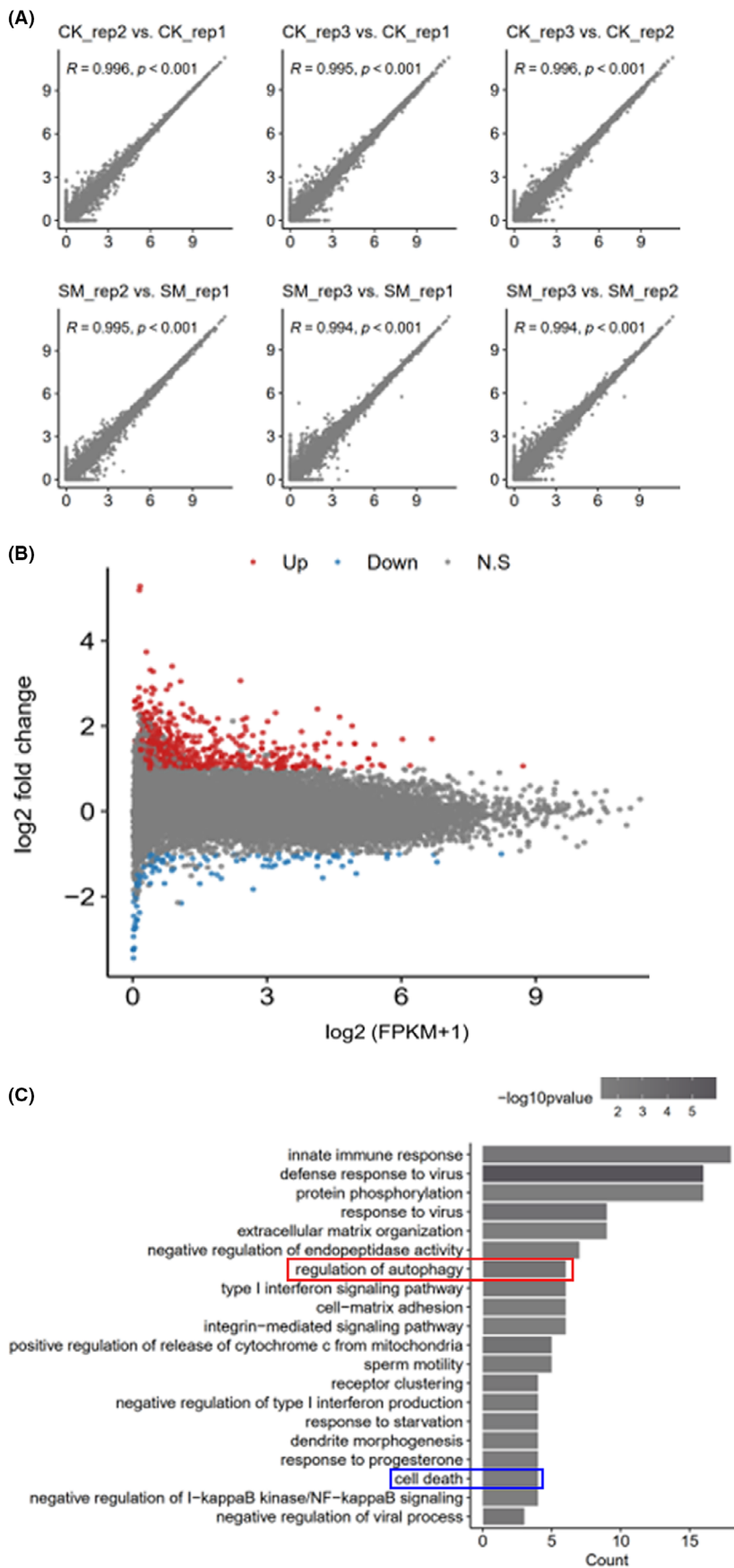


**FIGURE 3** Analysis of differential gene expression by RNA-seq data in solamargine (SM)-treated H929 cells. (A) Consistency across replicates of the RNA-seq experiment. (B) The gene expression level was measured based on reads per kilobase of transcript per million mapped reads (RPKM). (C) Gene Ontology (GO) analysis of differentially expressed genes in H929 cells exposed to SM (the genes with at least two-fold change of expression level were identified)

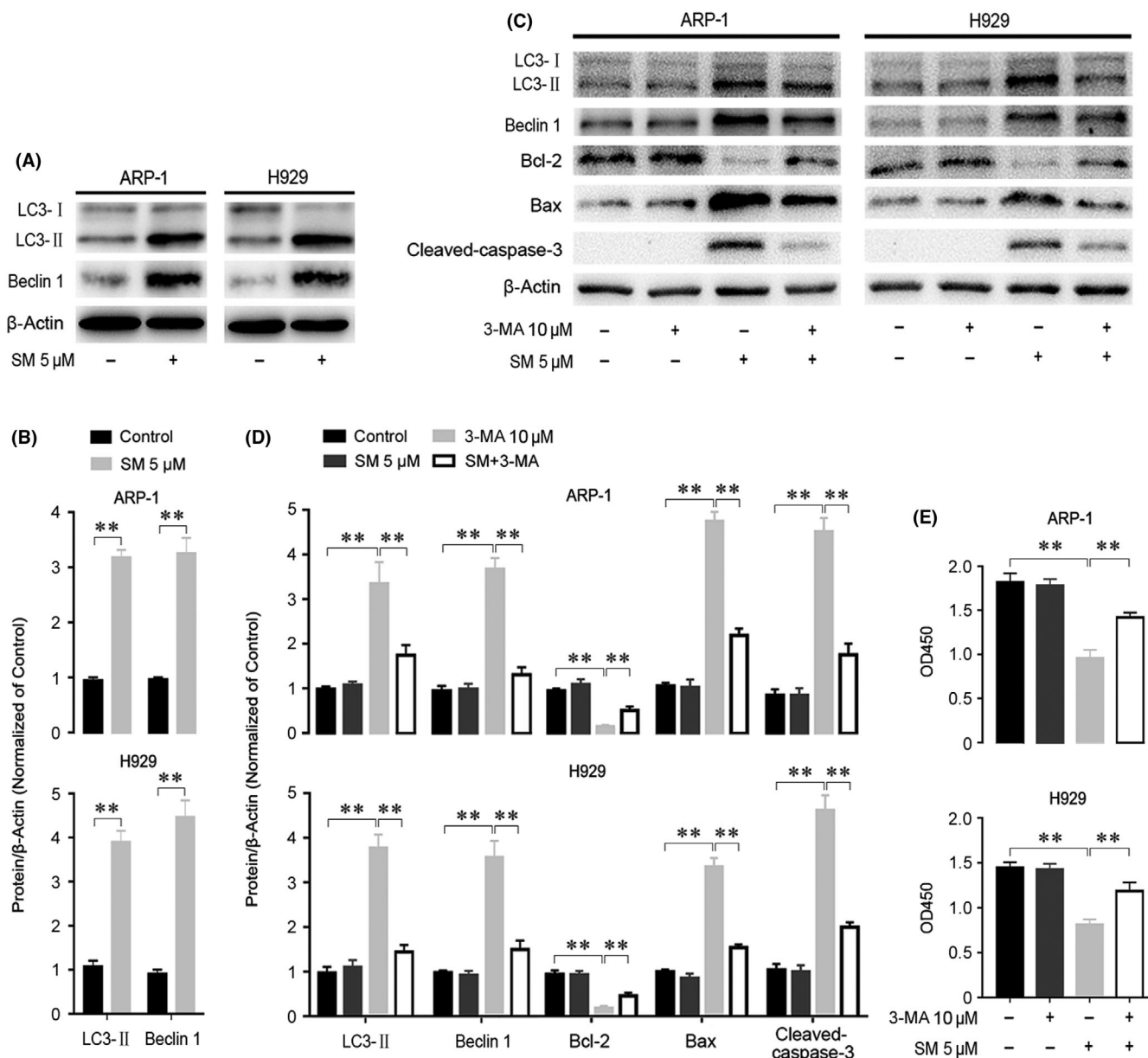


**FIGURE 4** Solamargine (SM) triggers activation of autophagy contributing to MM-cell apoptosis. ARP-1 and H929 cells were treated with SM (5 μM) for 24 h, or pretreated with/without 3-MA (10 μM) for 2 h and then exposed to SM (5 μM) for 24 h. (A) and (C) Total cell lysates were subjected to Western blotting using indicated antibodies. The blots were probed for β-tubulin as a loading control. Similar results were observed in three independent experiments. (B) and (D) The blots for LC3-II, Beclin 1, Bcl-2, Bax and cleaved-caspase-3 were semi-quantified. (E) The OD values at 450 nm were assessed using CCK-8 assay. For (B), (D) and (E), all data were expressed as means ± SD (n = 3–5, \*\*p < 0.01)

the detrimental effects of SM on MM cells is largely owing to an excessive activation of autophagy.

## 2.4 | SM in combination with BTZ shows greater anti-MM efficacy in vitro

BTZ is a proteasome inhibitor that is commonly used in the systematic treatment of MM. Owing to the often beneficial results observed when drugs are used in combination, we therefore examined whether the combination of SM with BTZ exhibits greater anti-MM activity than either

agent alone. To test this, combinations of different concentrations of SM and BTZ were investigated, and the combination index (CI) values were calculated using the CompuSyn software as mentioned in Methods. This analysis identified synergistic effects between SM and BTZ in ARP-1 and H929 cells (Figure 5A). To confirm the efficacy of this SM-BTZ combination, MM cells were cultured with 5 nM BTZ for 24 h with or without pre-treatment of 5 μM SM. Using a live cell assay, we found that SM enhanced the reduced viability caused by BTZ (Figure 5B). To examine the effects of this combination on primary MM cells, we cultured primary human bone marrow mononuclear cells (BM-MNCs) obtained from newly diagnosed MM patients for 24 h with or without 5 nM BTZ in the

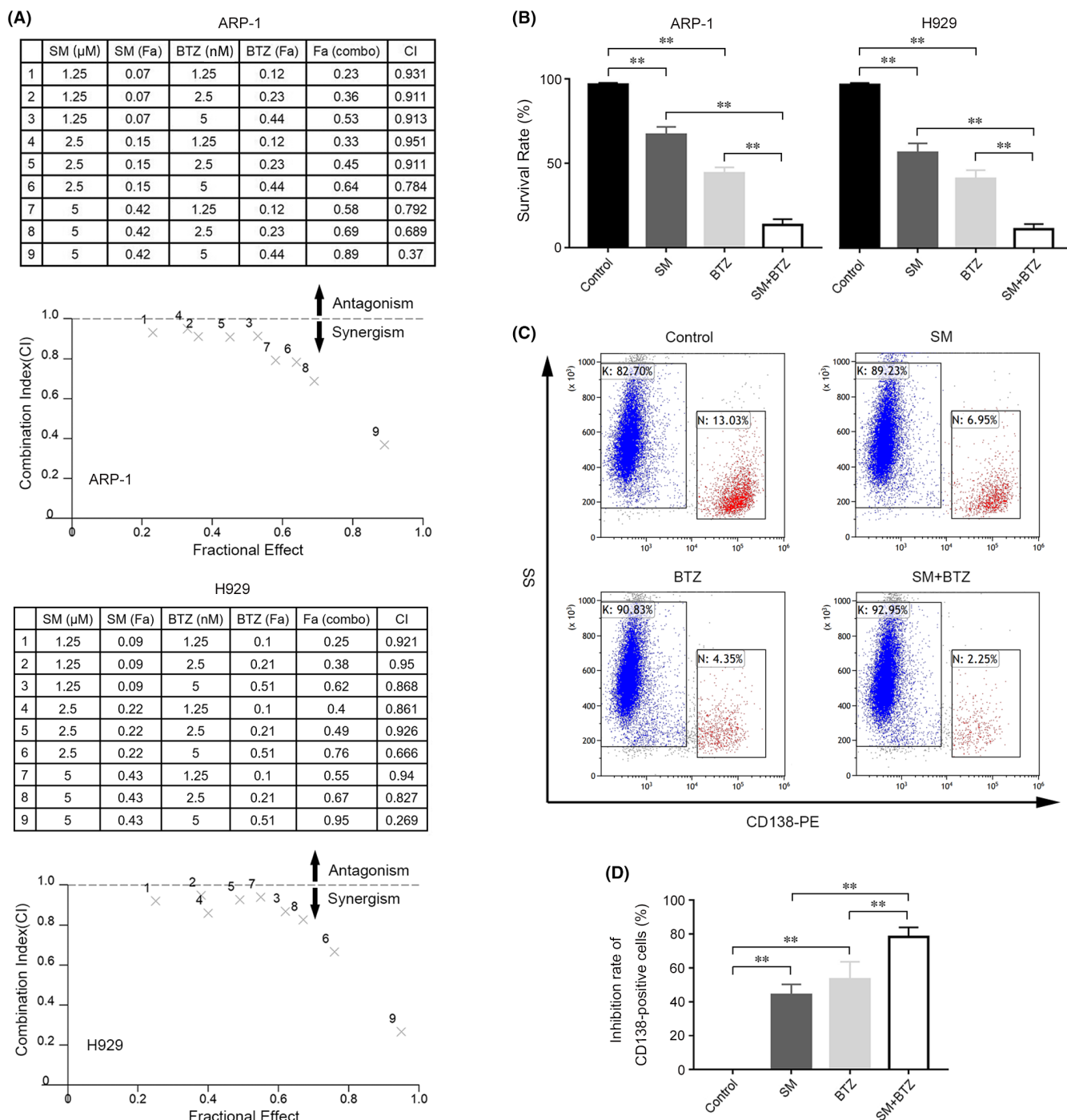


**FIGURE 5** Solamargine (SM) combined with Bortezomib (BTZ) shows a synergistic anti-MM effect in ARP-1 and H929 cells. (A) Combination index of SM and BTZ. ARP-1 and H929 cells were treated 24 h across a range of concentrations of SM, BTZ or SM plus BTZ, and measured for cell viability using CCK-8 assay. Combination index (CI) values corresponding to the specified data points on the table were obtained using CompuSyn software program for non-constant drug ratio and plotted on the graph against fraction effect (Fa) to assess SM-BTZ synergy. A CI < 1 indicates synergism. (B) ARP-1 and H929 cells were treated with SM (5  $\mu$ M), BTZ (5 nM) or SM (5  $\mu$ M) plus BTZ (5 nM), live cells were detected by counting viable cells using trypan blue exclusion. (C) and (D) Primary BM-MNCs obtained from newly diagnosed MM patients were treated with SM (5  $\mu$ M) or BTZ (5 nM) for 24 h, alone or in combination, the percentage of CD138<sup>+</sup> cells in each group were determined by flow cytometry. For (B) and (D), all data were expressed as means  $\pm$  SD ( $n = 3-5$ , \*\* $p < 0.01$ )

presence or absence of 5  $\mu$ M SM, and measured the percentages of CD138<sup>+</sup> cells in each group by flow cytometry. This experiment showed that each of SM and BTZ, alone, decreased the percentage of CD138<sup>+</sup> cells, whereas the combination of SM with BTZ reduced CD138<sup>+</sup> cells to

an even lower level (Figure 5C and D), suggesting that the combined efficacy of SM plus BTZ is greater than that of either individual treatment alone. These findings clearly demonstrate a remarkable synergy of SM and BTZ in vitro.

## 2.5 | SM potentiates the inhibitory effect of BTZ on MM progression in vivo

Having shown the potential anti-MM effect of SM and BTZ combination in vitro, we next investigated its effect in vivo using a MM xenograft NOD/SCID mouse model. H929 xenograft mice were randomised to receive four different treatments, as indicated in Figure 6A. Consistent with the in vitro observations, the combination of SM with BTZ caused a greater reduction in tumour growth than either single agent treatment alone (Figure 6A). As shown in Figure 6B and C, after four consecutive treatments, the tumour size and weight were clearly decreased after treatment with SM or BTZ alone, compared with untreated control. Notably, the volumes and weights of the tumours were much lower in the group treated with BTZ plus SM (Figure 6B and C). Moreover, we observed that the density of tumour cells and Ki-67 expression were strikingly decreased in tumour sections of SM- and BTZ-treated mice, as determined by HE and immunohistochemical staining, respectively (Figure 6D). The combined treatment of SM and BTZ induced a further reduction in both the density of tumour cells and the expression of Ki-67 in tumour tissues (Figure 6D). Of note, we observed a slight decrease in body weight in the mice treated with BTZ, whereas there was no significant difference in body weight between the SM treatment group and control, nor between the mice treated with the SM-BTZ combination and those treated with BTZ alone (Figure 6E). Thus, taken together, these in vivo data further demonstrate the efficacy of SM in inhibiting the

growth of MM as well as potent synergistic effects with BTZ, and indicate no significant toxicity caused by SM.

## 3 | DISCUSSION

There is presently a great need for novel therapeutic options in the treatment of MM owing to the poor survival rate of MM patients.<sup>2,3</sup> In this study, we explored the potential of SM, a component of the Chinese traditional herb *Solanum nigrum* L., for its effects on MM cells both in vitro and in vivo. We demonstrated that, by inducing excessive autophagy, SM produces a significant inhibitory effect on the viability of MM cells. Importantly, we showed a strong anti-proliferative/survival activity of SM combined with BTZ against MM both in vitro and in vivo.

Natural products have been documented to exhibit many similarities to known metabolites as well as high levels of bioavailability.<sup>6</sup> Additionally, natural phytochemicals exert low, or even no, toxicity to healthy cells, and some have good pharmacokinetic properties.<sup>20</sup> Due to these factors, studies that report the potent effects of natural phytochemicals on cancers have increased dramatically in the last few decades.<sup>6</sup> Several studies have indicated that SM, a natural phytochemical component, is a promising anti-tumour drug in a variety of solid malignancies, including melanoma cancer, gastric cancer, pancreatic cancer, lung cancer and nasopharyngeal carcinoma.<sup>10-12,21,22</sup> In this work, we build on these observations and show that SM also

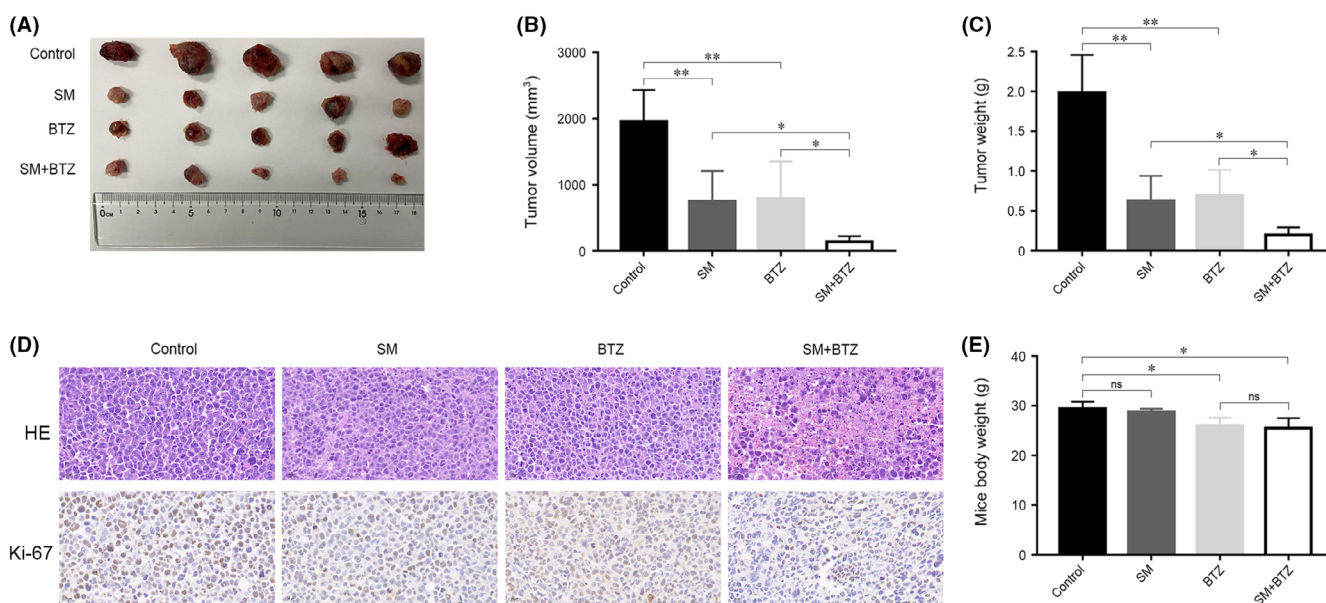


**FIGURE 6** Solamargine (SM) enhances the antitumor efficacy of bortezomib (BTZ) in MM xenograft mouse models. H929 cells ( $3 \times 10^6$ ) were injected subcutaneously into the right flanks of male NOD/SCID mice. When the tumour volume reached nearly 100 mm<sup>3</sup>, the mice were randomised divided into four groups, and treated with vehicle or SM (8 mg/kg) and/or BTZ (1 mg/kg) weekly for 4 weeks. Mice were killed after four consecutive treatment procedures. (A) Tumours were isolated and photographed. (B) and (C) Tumour volume and weight were measured. (D) Representative images of haematoxylin and eosin (HE) and immunohistochemical staining for Ki-67 in the subcutaneous tumours of four groups. The magnifications are 40 $\times$ . (E) Mouse body weight was measured. For (B, C and E), all data were expressed as means  $\pm$  SD (n = 5, \* $p$  < 0.05, \*\* $p$  < 0.01)

exhibits an anti-MM effect, dramatically inhibiting cell viability and inducing apoptosis in ARP-1 and H929 cells (Figure 2) as well as suppressing MM progression in vivo (Figure 6). Of note, there was no significant change in body weight of SM-treated mice compared with controls (Figure 6E), indicating that there is no significant toxicity of SM. These findings establish SM as a significantly promising drug option for the treatment of MM.

Prior work has demonstrated a bidirectional role of autophagy in the pathophysiology of MM and in myeloma cells.<sup>17,23</sup> Emerging evidence has revealed that plasma cells heavily rely on autophagy during the differentiation of B cells.<sup>23,24</sup> A specific level of autophagy is necessary for myeloma cells to sustain life.<sup>23,24</sup> Hence, inhibiting autophagy is considered to be a potentially effective strategy against MM.<sup>25</sup> In most cases, autophagy plays an anti-apoptotic role by raising the stress threshold required for the induction of apoptosis, or by directly suppressing apoptosis.<sup>17,26,27</sup> However, in rare cases, excessive autophagy can lead to ACD of tumour cells due to the extreme degradation of the organelles and cytoplasm.<sup>28,29</sup> In the present study, using RNA-seq, we found that autophagy-related genes were transcriptionally activated by SM in H929 cells (Figure 3C). Consistent with this, Western blotting analysis showed that SM markedly enhanced the levels of autophagy-associated proteins, LC3-II and Beclin 1, in both ARP-1 and H929 cells (Figure 4A and B). These results indicate that, unlike most cases, SM activates autophagy, rather than inhibits it, in MM cells. Moreover, inhibition of autophagy with 3-MA antagonised SM-induced apoptosis and suppression of viability in the cells (Figure 4C–E), indicating autophagy activation as an important contributor of SM-induced anti-MM activity. Clinically, various autophagic inhibitors, such as chloroquine, hydroxychloroquine and luanthone, have been explored for cancer therapy.<sup>30</sup> Our study provides a contrary view whereby SM can be used as an autophagic activator in the treatment of MM. Of note, using SymMap, we predicted several potential targets of SM, including ABCG2, Bcl-2, PTEN, and RB1 (Figure 1B). We then provided evidence that one of the predicted targets Bcl-2 was indeed downregulated by SM in MM cells (Figure 2E and F). Bcl-2 plays a crucial role in autophagy inhibition by binding to Beclin 1 to impede autophagy induction.<sup>25,31</sup> Thus, it is possible that SM enhances autophagy by suppressing the level of Bcl-2 in MM cells. In solid tumours, non-coding RNAs including long non-coding RNAs and microRNAs play an important role in SM-suppressed tumour progression.<sup>10–12</sup> Numerous studies have revealed that non-coding RNAs participate in malignancy formation, progression, and metastasis in MM.<sup>32–34</sup> We thus speculate that non-coding RNAs may contribute to the excessive autophagy-mediated inhibition of MM cells exposed to SM, a possibility that remains to be further investigated.

Among first-line agents in the clinical treatment of MM, the proteasome inhibitor BTZ has significantly improved patient outcomes.<sup>25</sup> However, the current clinical issues with the use of BTZ are drug resistance and relapse. To improve response rates, prolong response and delay the onset of drug resistance, therapeutic combinations of BTZ with other agents have been frequently examined in pre-clinical studies and clinical MM therapy.<sup>25</sup> In this study, using the

CCK-8 assay and CompuSyn software, we observed synergistic effects on MM between SM and BTZ (Figure 5A). We also showed that the combination of SM plus BTZ was indeed more effective than either agent alone in MM cell lines (ARP-1 and H929) and human bone marrow CD138<sup>+</sup> primary myeloma cells (Figure 5B–D). These *in vitro* results were further confirmed in a MM xenograft mouse model (Figure 6), indicating that combining SM with BTZ increases tumour cytotoxicity and exhibits more significant anti-MM efficacy than either single agent alone. Interestingly, studies have validated that BTZ-elicited autophagy leads to drug resistance.<sup>35,36</sup> However, our study hinted that SM may sensitise MM cells to BTZ by further activating autophagy, suggesting that autophagy induction is a double-edged sword in the survival/growth/death of MM cells.

In summary, in this study, we have shown that SM, as a single agent, exhibits remarkable detrimental activity against MM at least partly by promoting autophagy, which provides a proof-of-principle for the potential clinical application of SM in the treatment of MM. We further demonstrated that the combination of SM with BTZ synergistically exerts a greater anti-MM effect *in vitro* as well as *in vivo*, with no significant toxicity of SM. Our results thus identify SM as a potential novel drug to treat MM with high efficiency and safety, and the combination of SM and BTZ as an additional promising therapeutic strategy against this disease. Finally, we note that, considering the marked capability of SM to combat a range of cancers shown in previous work, our present study further provides impetus to synthetic organic chemists to more deeply investigate the finer chemical details, and modification possibilities, of this natural alkaloid so as to produce even more potent therapeutic options against MM as well as other cancers.

## 4 | MATERIALS AND METHODS

### 4.1 | Chemicals and antibodies

Solamargine was purchased from TargetMol (batch:117797, purity: 99.76%, Boston, MA, USA), whereas BTZ was provided by Med-ChemExpress (Shanghai, China). 3-MA was from Sigma (St Louis, MO, USA). RPMI 1640 medium and fetal bovine serum were from Gibco (Rockville, MD, USA). CCK-8 was supplied by Vazyme (Nanjing, China). The following antibodies were used: LC3, Beclin 1 and  $\beta$ -actin (Sigma), Bcl-2, Bax, cleaved-caspase-3 and Ki-67 (Cell Signalling Technology, Beverly, MA, USA), goat anti-rabbit IgG-horseradish peroxidase (HRP) and goat anti-mouse IgG-HRP (Pierce, Rockford, IL, USA). Other chemicals were of analytical grade and were purchased from local commercial sources.

### 4.2 | Cell lines and cell culture

Human MM cell lines ARP-1 and NCI-H929 (H929) were purchased from the Cell Bank of the Shanghai Institute of Biochemistry and Cell Biology, Chinese Academy of Sciences (Shanghai, China). Cells were

maintained in RPMI-1640 medium, supplemented with 10% FBS, 100 U/mL penicillin and 100 U/mL streptomycin (Hyclone, Logan, UT, USA), and cultured at 37 °C in a humidified incubator containing 5% CO<sub>2</sub>.

### 4.3 | Primary human bone marrow mononuclear cells (BM-MNCs) isolation and culture

Bone marrow aspirates were obtained from three newly diagnosed male patients with myeloma who signed informed consent in Jingjiang People's Hospital. All procedures performed in the present study involving human bone marrow aspirates were in accordance with the ethical standards of the Ethics Committee of Jingjiang People's Hospital (Approval number: 2021-05-016) and with the Declaration of Helsinki (as revised in Brazil in 2013).

BM-MNCs were isolated from the bone marrow aspirates by density gradient centrifugation using the Ficoll-Hypaque technique (Ficoll-Paque PLUS; GE Healthcare Bio-Sciences AB, Björkgatan, Uppsala, Sweden). BM-MNCs were maintained in *x-vivo* 15 medium (Lonza, Switzerland) and cultured at 37 °C in a humidified incubator containing 5% CO<sub>2</sub>.

### 4.4 | Analysis for cell viability

ARP-1 and H929 cells, seeded at a density of  $1 \times 10^4$  cells/well in 96-well plates, were treated with SM (0–10 μM for ARP-1 or 0–12 μM for H929) for 24 h, or with 5 μM SM for 0–48 h, or with/without 5 μM SM following pre-incubation with/without 3-MA (10 μM) for 2 h, with five replicates of each treatment. Subsequently, cell viability and the OD values at 450 nm were assessed by CCK-8 assay using a Victor X3 Light Plate Reader (PerkinElmer, Waltham, MA, USA).

### 4.5 | Live cell assay by trypan blue exclusion

ARP-1 and H929 cells, seeded in 6-well plates at a density of  $2 \times 10^5$  cells per well, were treated with/without SM (5 μM) and/or BTZ (5 nM) for 24 h, with five replicates of each treatment. Subsequently, live cells were monitored by counting viable cells using trypan blue exclusion test.

### 4.6 | Flow cytometry analysis

ARP-1 and H929 cells, seeded at a density of  $2 \times 10^5$  cells/well in 6-well plates, were treated with/without SM (5 μM) for 24 h. Apoptotic cells were quantified using a fluorescence-activated cell sorter (FACS) Vantage SE flow cytometer (Beckman, CA, USA) after staining with Annexin V-FITC/PI staining kit (Vazyme Biotech Co., Ltd, Nanjing, China).

Primary BM-MNCs, isolated from the bone marrow of newly diagnosed MM patients, were treated with/without SM (5 μM) and/or BTZ (5 nM) for 24 h. After incubation with conjugated antibody CD138-PE (Beckman Coulter Immunotech, Marseille, France) for 15 min, the percentage of CD138+ cells was analysed under a FACS Vantage SE flow cytometer (Beckman Coulter, Fullerton, CA, USA).

### 4.7 | Western blot analysis

ARP-1 and H929 cells were washed with cold phosphate buffered saline after treatment, and then lysed on ice with RIPA buffer (Beyotime, Shanghai, China). Lysates were sonicated for 10 s and centrifuged at  $16,000 \times g$  for 2 min at 4 °C. The supernatants were collected, and Western blotting was subsequently performed as described previously.<sup>37</sup> In brief, lysates containing equivalent quantities of protein were separated on a 10–12% SDS-polyacrylamide gels, and transferred to polyvinylidene difluoride membranes (Millipore, Bedford, MA, USA). Membranes were incubated with phosphate buffered saline containing 0.05% Tween 20 and 5% non-fat dry milk to block nonspecific binding, and then with primary antibodies against LC3, Beclin 1, Bcl-2, Bax and cleaved-caspase-3 overnight at 4 °C, respectively, followed by incubating with appropriate secondary antibodies including horseradish peroxidase-coupled goat anti-rabbit IgG or goat anti-mouse IgG overnight at 4 °C. Immunoreactive bands were visualised using enhanced chemiluminescence solution (Sciben Biotech Company, Nanjing, China). The blots for detected proteins were semi-quantified using NIH Image J software (National Institutes of Health, Bethesda, MD, USA).

### 4.8 | RNA-seq library construction and data analysis

Total RNA of both control and SM-treated H929 samples was extracted using Trizol (Life Technologies, Thermo Fisher Scientific, Waltham, MA, USA) according to the manufacturer's protocol. mRNA was isolated and then treated with DNase to remove residual genomic DNA. One hundred nanograms mRNA of each sample were used as starting material and the RNA-seq library was constructed with NEB-Next Ultra Directional RNA Library Prep Kit (NEB, Ipswich, MA, USA). Each sample was amplified with 12–14 cycles in a thermal cycler, using Q5 High-Fidelity DNA Polymerase (NEB). The PCR product was purified and subjected to Illumina sequencer. The raw sequencing data of this study are available in the EMBL database under accession number E-MTAB-10816: <http://www.ebi.ac.uk/arrayexpress/>.

The quality of raw sequence reads was examined by FastQC software. All qualified sequence reads were mapped to a reference genome (hg19) by TopHat.<sup>38</sup> Cufflinks was used to characterise the differential transcription pattern.<sup>38</sup> Gene expression level was measured by the reads per kilobase of transcript per million reads mapped (RPKM). For differential gene expression analysis, we identified the genes whose gene expression level saw at least a two-fold change.

The list of differentially expressed genes was uploaded to DAVID Bioinformatics Resources 6.7 and we performed analysis of the gene ontology (GO) cluster.

#### 4.9 | Multiple myeloma xenograft mouse model

Male NOD/SCID mice (five weeks old, 20–22 g) were obtained from the Vital River Laboratory Animal Technology Co., Ltd. (Beijing, China), and housed in the Animal Research Facility of Nanjing Drum Tower Hospital. H929 cells ( $3 \times 10^6$ ) were subcutaneously injected into the right flank of each mouse. When the established tumours reached a volume of approximately  $100 \text{ mm}^3$ , 20 mice were randomly divided into four groups (5 mice for each group) and injected with vehicle (control group), SM (8 mg/kg), BTZ (1 mg/kg) or SM plus BTZ (8 mg/kg plus 1 mg/kg) weekly for 4 weeks. Mice were killed after four consecutive treatment procedures. The tumours were removed, photographed and weighed. Tumour volume ( $\text{mm}^3$ ) was calculated with calliper using the formula: tumour volume =  $0.5 \times (\text{length} \times \text{width}^2)$ . All experiments were approved by the Ethics Committee of Animal Research of Nanjing Drum Tower Hospital Clinical College of Nanjing University of Chinese Medicine (Approval number: 2020AE01095).

#### 4.10 | Immunohistochemistry

Paraffin-embedded sections of tumour tissues from xenograft mice were incubated with an antibody directed against Ki-67 at  $4^\circ\text{C}$  overnight. Subsequently, the sections were treated with polymer, developed with DAB-Chromogen, and counterstained with haematoxylin, followed by imaging under a fluorescence microscopy (Leica DMI8, Wetzlar, Germany).

#### 4.11 | Statistical analysis

All data were expressed as mean  $\pm$  SD and calculated using Graphpad 8.0 (San Diego, CA, USA). One way analysis of variance followed by the Tukey's Post-hoc test were employed for statistical analysis. Differences with p-values less than 0.05 were considered statistically significant. Drug Synergy was quantified according to the Chou-Talalay Method for non-constant drug combination using the CalcuSyn software program (ComboSyn Inc., Paramus, NJ, USA).<sup>39</sup> A combination index (CI)  $>1.0$  suggested antagonistic effect, a CI = 1 suggested additive effect, and a CI  $<1$  suggested synergistic effect.

#### ACKNOWLEDGEMENTS

We express our great appreciation and gratitude to those MM patients who donated their bone marrow aspirates to this study. We thank Professor Czajkowsky for English language editing.

This study was supported by grants from the National Natural Science Foundation of China (82000215), the Jiangsu Provincial

Medical Innovation Team (CXTDA2017046), the Natural Science Foundation of Jiangsu Province (BK20210028) and the Nanjing Medical Science and Technique Development Foundation (YKK20083).

#### CONFLICT OF INTERESTS

The authors declare no competing interests.

#### AUTHOR CONTRIBUTIONS

Conceptualisation: Xiaoqing Dong and Bing Chen; Formal analysis: Qiaoyan Han and Xiaoqing Dong; Funding acquisition: Hua Bai, Xiaoqing Dong and Bing Chen; Investigation: Qiaoyan Han, Hua Bai and Yong Xu; Methodology: Qiaoyan Han and Yong Xu; Project administration: Bing Chen; Resources: He Zhou; Supervision: Bing Chen; Validation: Min Zhou; Writing – original draft: Qiaoyan Han; Writing – review & editing: Xiaoqing Dong.

#### DATA AVAILABILITY STATEMENT

The raw sequencing data of this study are available in the EMBL database under 435 accession number E-MTAB-10816: <http://www.ebi.ac.uk/arrayexpress/>. The other data presented in this study are included in the article or available from the corresponding authors, Xiaoqing Dong or Bing Chen, upon reasonable request.

#### ORCID

Xiaoqing Dong  <https://orcid.org/0000-0002-1467-7886>

Bing Chen  <https://orcid.org/0000-0001-8303-2531>

#### REFERENCES

1. Joshua DE, Bryant C, Dix C, Gibson J, Ho J. Biology and therapy of multiple myeloma. *Med J Aust.* 2019;210:375-380.
2. Kazandjian D. Multiple myeloma epidemiology and survival: a unique malignancy. *Semin Oncol.* 2016;43:676-681.
3. Siegel RL, Miller KD, Jemal A. Cancer statistics, 2020. *CA Cancer J Clin.* 2020;70:7-30.
4. Bobin A, Liuu E, Moya N, et al. Multiple Myeloma: an overview of the current and novel therapeutic approaches in 2020. *Cancers (Basel).* 2020;12:2885.
5. Pinto V, Bergantim R, Caires HR, Seca H, Guimaraes JE, Vasconcelos MH. Multiple Myeloma: available therapies and causes of drug resistance. *Cancers (Basel).* 2020;12:407.
6. Kang B, Park H, Kim B. Anticancer activity and underlying mechanism of phytochemicals against multiple myeloma. *Int J Mol Sci.* 2019;20:2302.
7. Cicconi L, Platzbecker U, Avvisati G, et al. Long-term results of all-trans retinoic acid and arsenic trioxide in non-high-risk acute promyelocytic leukemia: update of the APL0406 Italian-German randomized trial. *Leukemia.* 2020;34:914-918.
8. Roschewski M, Dunleavy K, Abramson JS, et al. Multicenter study of risk-adapted therapy with dose-adjusted EPOCH-R in adults with untreated Burkitt lymphoma. *J Clin Oncol.* 2020;38:2519-2529.
9. Zhang Z, Jiang M, Borthakur G, et al. Acute myeloid leukemia with a novel CPSF6-RARG variant is sensitive to homoharringtonine and cytarabine chemotherapy. *Am J Hematol.* 2020;95:E48-E51.
10. Fu R, Wang X, Hu Y, et al. Solamargine inhibits gastric cancer progression by regulating the expression of IncNEAT1\_2 via the MAPK signaling pathway. *Int J Oncol.* 2019;54:1545-1554.
11. Tang Q, Zheng F, Liu Z, et al. Novel reciprocal interaction of lncRNA HOTAIR and miR-214-3p contribute to the solamargine-inhibited

- PDPK1 gene expression in human lung cancer. *J Cell Mol Med.* 2019;23:7749-7761.
12. Wu J, Tang X, Ma C, Shi Y, Wu W, Hann SS. The regulation and interaction of colon cancer-associated transcript-1 and miR7-5p contribute to the inhibition of SP1 expression by solamargine in human nasopharyngeal carcinoma cells. *Phytother Res.* 2020;34:201-213.
  13. Levine B, Kroemer G. Autophagy in the pathogenesis of disease. *Cell.* 2008;132:27-42.
  14. Choi AM, Rytter SW, Levine B. Autophagy in human health and disease. *N Engl J Med.* 2013;368:651-662.
  15. White E. Deconvoluting the context-dependent role for autophagy in cancer. *Nat Rev Cancer.* 2012;12:401-410.
  16. Galluzzi L, Vitale I, Abrams JM, et al. Molecular definitions of cell death subroutines: recommendations of the nomenclature committee on cell death 2012. *Cell Death Differ.* 2012;19:107-120.
  17. Yun Z, Zhichao J, Hao Y, et al. Targeting autophagy in multiple myeloma. *Leuk Res.* 2017;59:97-104.
  18. Desantis V, Saltarella I, Lamanuzzi A, et al. Autophagy: a new mechanism of Prosurvival and drug resistance in multiple myeloma. *Transl Oncol.* 2018;11:1350-1357.
  19. Wu Y, Zhang F, Yang K, et al. SymMap: an integrative database of traditional Chinese medicine enhanced by symptom mapping. *Nucleic Acids Res.* 2019;47:D1110-D1117.
  20. Pojero F, Poma P, Spano V, Montalbano A, Barraja P, Notarbartolo M. Targeting multiple myeloma with natural polyphenols. *Eur J Med Chem.* 2019;180:465-485.
  21. Al Sinani SS, Eltayeb EA, Coomber BL, Adham SA. Solamargine triggers cellular necrosis selectively in different types of human melanoma cancer cells through extrinsic lysosomal mitochondrial death pathway. *Cancer Cell Int.* 2016;16:11.
  22. Xie X, Zhang X, Chen J, et al. Fe3O4-solamargine induces apoptosis and inhibits metastasis of pancreatic cancer cells. *Int J Oncol.* 2019;54:905-915.
  23. Carroll RG, Martin SJ. Autophagy in multiple myeloma: what makes you stronger can also kill you. *Cancer Cell.* 2013;23:425-426.
  24. Pengo N, Scolari M, Oliva L, et al. Plasma cells require autophagy for sustainable immunoglobulin production. *Nat Immunol.* 2013;14:298-305.
  25. Roy M, Liang L, Xiao X, et al. Lycorine Downregulates HMGB1 to inhibit autophagy and enhances Bortezomib activity in multiple myeloma. *Theranostics.* 2016;6:2209-2224.
  26. Li A, Chen X, Jing Z, Chen J. Trifluoperazine induces cellular apoptosis by inhibiting autophagy and targeting NUPR1 in multiple myeloma. *FEBS Open Bio.* 2020;10:2097-2106.
  27. Wang G, Zhou P, Chen X, et al. The novel autophagy inhibitor elaiophyllin exerts antitumor activity against multiple myeloma with mutant TP53 in part through endoplasmic reticulum stress-induced apoptosis. *Cancer Biol Ther.* 2017;18:584-595.
  28. Zheng Z, Wang L, Cheng S, Wang Y, Zhao W. Autophagy and myeloma. *Adv Exp Med Biol.* 2020;1207:625-631.
  29. Ikeda S, Abe F, Matsuda Y, Kitadate A, Takahashi N, Tagawa H. Hypoxia-inducible hexokinase-2 enhances anti-apoptotic function via activating autophagy in multiple myeloma. *Cancer Sci.* 2020;111:4088-4101.
  30. Carew JS, Kelly KR, Nawrocki ST. Autophagy as a target for cancer therapy: new developments. *Cancer Manag Res.* 2012;4:357-365.
  31. Fernandez AF, Sebti S, Wei Y, et al. Disruption of the beclin 1-BCL2 autophagy regulatory complex promotes longevity in mice. *Nature.* 2018;558:136-140.
  32. Adamia S, Abiatari I, Amin SB, et al. The effects of MicroRNA deregulation on pre-RNA processing network in multiple myeloma. *Leukemia.* 2020;34:167-179.
  33. Ding T, Deng R, Huang T. Long non-coding RNA T cell factor 7 is associated with increased disease risk and poor prognosis, and promotes cell proliferation, attenuates cell apoptosis and miR-200c expression in multiple myeloma. *Oncol Lett.* 2021;21:129.
  34. He YQ, Zhang ZY, Zhou HX, Ye F, Chen WM. Competing endogenous RNA network in newly diagnosed multiple myeloma by genetic microarray. *Chin Med J (Engl).* 2020;133:2619-2621.
  35. Escalante AM, McGrath RT, Karolak MR, Dorr RT, Lynch RM, Landowski TH. Preventing the autophagic survival response by inhibition of calpain enhances the cytotoxic activity of bortezomib in vitro and in vivo. *Cancer Chemother Pharmacol.* 2013;71:1567-1576.
  36. Jagannathan S, Abdel-Malek MA, Malek E, et al. Pharmacologic screens reveal metformin that suppresses GRP78-dependent autophagy to enhance the anti-myeloma effect of bortezomib. *Leukemia.* 2015;29:2184-2191.
  37. Zhang H, Dong X, Zhao R, et al. Cadmium results in accumulation of autophagosomes-dependent apoptosis through activating Akt-impaired autophagic flux in neuronal cells. *Cell Signal.* 2019;55:26-39.
  38. Trapnell C, Roberts A, Goff L, et al. Differential gene and transcript expression analysis of RNA-seq experiments with TopHat and cufflinks. *Nat Protoc.* 2012;7:562-578.
  39. Chou TC. Theoretical basis, experimental design, and computerized simulation of synergism and antagonism in drug combination studies. *Pharmacol Rev.* 2006;58:621-681.

**How to cite this article:** Han Q, Bai H, Xu Y, et al. Solamargine induces autophagy-mediated apoptosis and enhances bortezomib activity in multiple myeloma. *Clin Exp Pharmacol Physiol.* 2022;49(6):674-685. doi:10.1111/1440-1681.13643